

Searches for Population III pair-instability supernovae: Predictions for ULTIMATE-Subaru and WFIRST

Takashi J. MORIYA¹, Kenneth C. WONG^{2,1}, Yusei KOYAMA³, Masaomi TANAKA⁴, Masamune OGURI^{5,6,2}, Stefan HILBERT^{7,8} and Ken'ichi NOMOTO²

¹Division of Theoretical Astronomy, National Astronomical Observatory of Japan, National Institutes of Natural Sciences, 2-21-1 Osawa, Mitaka, Tokyo 181-8588, Japan

²Kavli Institute for the Physics and Mathematics of the Universe (WPI), The University of Tokyo Institutes for Advanced Study, The University of Tokyo, 5-1-5 Kashiwanoha, Kashiwa, Chiba 277-8583, Japan

³Subaru Telescope, National Astronomical Observatory of Japan, National Institutes of Natural Sciences, 650 North A'ohoku Place, Hilo, HI 96720, USA

⁴Astronomical Institute, Tohoku University, 6-3 Aramaki Aza-Aoba, Aoba-ku, Sendai 980-8578, Japan

⁵Research Center for the Early Universe, Graduate School of Science, The University of Tokyo, 7-3-1 Hongo, Bunkyo, Tokyo 113-0033, Japan

⁶Department of Physics, Graduate School of Science, The University of Tokyo, 7-3-1 Hongo, Bunkyo, Tokyo 113-0033, Japan

⁷Exzellenzcluster Universe, Boltzmannstr. 2, D-85748 Garching, Germany

⁸Ludwig-Maximilians-Universität, Universitäts-Sternwarte, Scheinerstr. 1, D-81679 München, Germany

*E-mail: takashi.moriya@nao.ac.jp

Received 18-Jan-2019; Accepted 02-Mar-2019

Abstract

ULTIMATE-Subaru (Ultra-wide Laser Tomographic Imager and MOS with AO for Transcendent Exploration on Subaru) and WFIRST (Wide Field Infra-Red Survey Telescope) are the next generation near-infrared instruments that have a large field-of-view. They allow us to conduct deep and wide transient surveys in near-infrared. Such a near-infrared transient survey enables us to find very distant supernovae that are redshifted to the near-infrared wavelengths. We have performed the mock transient surveys with ULTIMATE-Subaru and WFIRST to investigate their ability to discover Population III pair-instability supernovae. We found that a 5-year 1 deg^2 K -band transient survey with the point-source limiting magnitude of 26.5 mag with ULTIMATE-Subaru may find about 2 Population III pair-instability supernovae beyond the redshift of 6. A 5-year 10 deg^2 survey with WFIRST reaching 26.5 mag in the $F184$ band may find about 7 Population III pair-instability supernovae beyond the redshift of 6. We also find that the expected numbers of the Population III pair-instability supernova detections increase about a factor of 2 if the near-infrared transient surveys are performed towards clusters of galaxies. Other supernovae such as Population II pair-instability supernovae would also be detected in the same survey. This study demonstrates that the future wide-field near-infrared instruments allow us to investigate the explosions of the first generation supernovae by performing the deep and wide near-infrared transient surveys.

Key words: supernovae: general — stars: massive — stars: Population III

1 Introduction

The last decade encountered the great success of optical transient surveys. Many optical transient surveys such as PTF (Law et al. 2009), Pan-STARRS (Chambers et al. 2016), SkyMapper (Keller et al. 2007), KISS (Morokuma et al. 2014), and HSC (Tanaka et al. 2016, Moriya et al. 2019, Yasuda et al. submitted) have shown that stellar deaths have much more varieties than expected before. One of the most fascinating discoveries from these optical transient surveys are the discovery of very luminous supernovae (SNe) called superluminous supernovae (SLSNe, Quimby et al. 2011; see Moriya et al. 2018 for a review). They are often more than 10 times brighter than canonical SNe. Shortly after their discovery, it has been speculated that their huge luminosities could be due to massive production of radioactive ^{56}Ni and, therefore, SLSNe might be pair-instability SNe (PISNe) (e.g., Smith et al. 2007; Gal-Yam et al. 2009). PISNe are theoretically predicted explosions of very massive stars (Rakavy & Shaviv 1967; Barkat et al. 1967). PISNe could lead to the production of more than $10 M_{\odot}$ of ^{56}Ni (Heger & Woosley 2002), which is generally required to explain the huge luminosity of SLSNe.

Although PISNe were originally suggested to be a probable origin of SLSNe, it turned out that SLSNe generally show different observational properties than those expected from PISNe (e.g., Kasen et al. 2011; Dessart et al. 2012; Whalen et al. 2014; Jerkstrand et al. 2016; Tolstov et al. 2017 but see also Kozyreva et al. 2016). PISNe are a natural consequence of very massive stars that have the helium core masses between $\sim 70 M_{\odot}$ and $\sim 140 M_{\odot}$ (Langer 2012), and we would observe them if massive stars with such massive cores exist. Unfortunately, it is very hard to keep the cores massive enough to explode as PISNe until their deaths in the solar metallicity environment (e.g., Yoshida et al. 2014, but see also Georgy et al. 2017) and PISNe are suggested to occur when the metallicity is below one third of the solar metallicity (Langer et al. 2007). The most promising stars to explode as PISNe are the first stars, or Population III (Pop III) stars. Pop III stars do not suffer from wind mass loss and they can grow massive enough cores to explode as PISNe when their zero-age main-sequence (ZAMS) masses are between $\sim 140 M_{\odot}$ and $\sim 260 M_{\odot}$ (Heger & Woosley 2002; Umeda & Nomoto 2002). Pop III stars are also predicted to be dominated by massive stars including those in the PISN mass range (e.g., Hirano et al. 2015). Therefore, many Pop III stars are likely to explode as PISNe.

Pop III star formation could last until $z \sim 6$ (e.g., de Souza et al. 2014) and, therefore, we need to reach at least $z \sim 6$ to look

for Pop III PISNe. It is inevitable to perform transient surveys in near infrared (NIR) to search for transients at such high redshifts (e.g., Scannapieco et al. 2005; Tanaka et al. 2013; Whalen et al. 2013b; de Souza et al. 2013; Hartwig et al. 2018). Only a handful of NIR transient surveys are conducted in the last decade (e.g., Mattila et al. 2012; Kool et al. 2018; Kasliwal et al. 2017). However, many NIR wide field imaging instruments are currently planned and NIR transient surveys would be the frontier of transient surveys in the coming decade (e.g., Inserra et al. 2017; Hounsell et al. 2017). Among them, ULTIMATE-Subaru (Ultra-wide Laser Tomographic Imager and MOS with AO for Transcendent Exploration¹) and WFIRST (Wide-Field InfraRed Survey Telescope, Spergel et al. 2015) have a wide-field NIR imaging facility that is suitable to perform deep and wide NIR transient surveys. In this paper, we perform mock NIR transient surveys with ULTIMATE-Subaru and WFIRST to search for Pop III PISNe at $z \gtrsim 6$ and study optimal survey strategies to detect them. We also take the effect of the luminosity amplifications due to gravitational lensing into account (cf. Whalen et al. 2013a). In this paper, we focus on survey strategies and observational methods to discover Pop III PISNe and we briefly show the effect of the gravitational lensing in this paper. The details on how gravitational lensing could affect the survey results, as well as the details on how we estimate the gravitational lensing effect, are discussed in an accompanying paper by Wong et al. (2019).

The rest of this paper is organized as follows. We first present our method of mock observations in Section 2. We present our results of mock observations and discuss the optimal strategy to look for Pop III PISNe at $z \gtrsim 6$ in Section 3. We have general discussion of our results in Section 4 and conclude this paper in Section 5. Throughout this paper, we adopt the standard Λ CDM cosmology with $H_0 = 70 \text{ km s}^{-1} \text{ Mpc}^{-1}$, $\Omega_{\Lambda} = 0.7$, and $\Omega_M = 0.3$. All the magnitudes presented in this paper are in the AB magnitude system.

2 Set-up of mock observations

2.1 Instruments

We first introduce ULTIMATE-Subaru and WFIRST. The two instruments are complimentary to each other in terms of the wavelength coverage and the field-of-view (FoV).

¹ <https://www.naoj.org/Projects/newdev/ngao/>

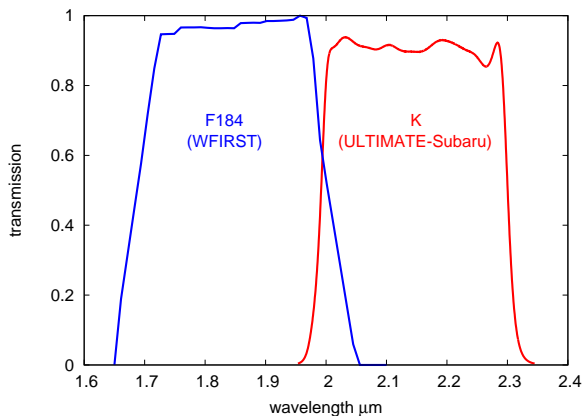


Fig. 1. Filters used in our SN survey simulations. The K -band filter assumed for ULTIMATE-Subaru is that currently used by Subaru/MOIRCS. The $F184$ filter is the reddest filter currently planned by WFIRST.

2.1.1 ULTIMATE-Subaru

ULTIMATE-Subaru is the next generation wide-field AO system with a wide-field NIR instrument. It is currently planned to have the NIR imager with the FoV of $14' \times 14'$ (0.054 deg^2). It requires 18.4 pointings to cover 1 deg^2 , for example.

The details of the instrument are still under discussion. The reddest band currently planned is the K band. We expect that the instrument specification such as filters and exposure time of ULTIMATE-Subaru will be similar to those of Multi-Object Infrared Camera and Spectrograph (MOIRCS) currently on Subaru (Suzuki et al. 2008; Ichikawa et al. 2006). We adopt the K band filter of MOIRCS in this study (Fig. 1). According to the exposure time calculator for MOIRCS², it takes 2.6 hours to reach the limiting magnitude (signal-to-noise ratio of 5 for a point source throughout this paper) of 26.0 mag in the K band with a standard condition ($0.2''$ seeing with $0.3''$ aperture). With the best expected condition, it is possible to reach $0.15''$ seeing. Then, the limiting magnitude of 26.5 mag in the K band can be reached in 4.6 hours.

2.1.2 WFIRST

WFIRST is the next generation space telescope with the wide-field imager that has the FoV of 0.28 deg^2 (Spergel et al. 2015). 3.6 pointings are required to cover 1 deg^2 .

The reddest filter for the imager currently planned is the $F184$ filter (Fig. 1) and we adopt it in this study. The deepest SN survey currently planned with WFIRST has the limiting magnitude of about 26.5 mag. It takes 0.5 hours to reach 26.5 mag in $F184$. The limiting magnitude of 26.0 mag can be reached in 0.2 hours. We also perform a simulation with the limiting magnitude of 27.0 mag, which can be reached in 1.3 hours.

2.2 Survey strategy

We perform our mock observation simulations with several different survey strategies. We fix our survey period to be 5 years. We only use one filter in our mock transient surveys, K for ULTIMATE-Subaru and $F184$ for WFIRST.

The survey field is assumed to be observed repeatedly with an interval of t_{int} . We also set the minimum number of detections N_d for a transient to be regarded as a discovery. For example, if we assume $N_d = 3$, PISNe detected more than 3 times are regarded as PISN discoveries. In this case, PISNe detected only two times are ignored.

For the ULTIMATE-Subaru survey, we assume two different limiting magnitudes, 26.5 mag and 26.0 mag in the K band. It requires about 70 hours to cover 1 deg^2 with 26.5 mag for one epoch. Assuming $t_{\text{int}} = 180$ days, the 5-year 1 deg^2 transient survey with the 26.5 mag limit takes 860 hours in total. If we adopt 26.0 mag as the survey limiting magnitude, it takes 48 hours to cover 1 deg^2 . With $t_{\text{int}} = 180$ days for 5 years, 480 hours and 960 hours are required to conduct the 1 deg^2 and 2 deg^2 surveys, respectively.

WFIRST requires 2 hours and 0.75 hours to cover 1 deg^2 with the limiting magnitude of 26.5 mag and 26.0 mag, respectively. For instance, the transient survey with $t_{\text{int}} = 180$ days covering 10 deg^2 in 5 years takes 200 hours (26.5 mag limit) and 75 hours (26.0 mag limit).

2.3 PISN properties

2.3.1 Light curves

We adopt PISN light curves (LCs) predicted by Kasen et al. (2011) for our observation simulations. The LCs are numerically obtained from the PISN progenitors of Heger & Woosley (2002). The peak luminosity of the R250 and He130 models (see the next paragraph for the description of the models) exceeds $K = 26.0$ mag at $z = 6$ (Fig. 2). The R225 and He120 models are brighter than 26.5 mag in the K band at $z = 6$ (Fig. 2). Thus, the R225 and He120 explosions at $z \gtrsim 6$ can only be observed when we conduct the transient surveys with the limiting magnitude of 26.5 mag in the K band. If we use the $F184$ filter, only R250 and R225 are brighter than 26.5 mag at the peak at $z \gtrsim 6$ (Fig. 2). For reference, the peak magnitude of the R250 model in the H band of WFIRST (Spergel et al. 2015) is around 27.1 mag and it is much more efficient to conduct a survey in the $F184$ band. The $F184$ band magnitudes become significantly faint in He130 and He120 models because the helium core models are redder than the red supergiant models. For example, the synthetic spectra of R250 at around the maximum luminosity peak at $\sim 2500 \text{ \AA}$, while the helium core models peak at $\sim 3500 \text{ \AA}$ (Kasen et al. 2011). This difference likely originates from the difference in Fe-group absorption. The red supergiant models have the photosphere in their hydrogen-rich

² https://www.naoj.org/cgi-bin/img_etc.cgi

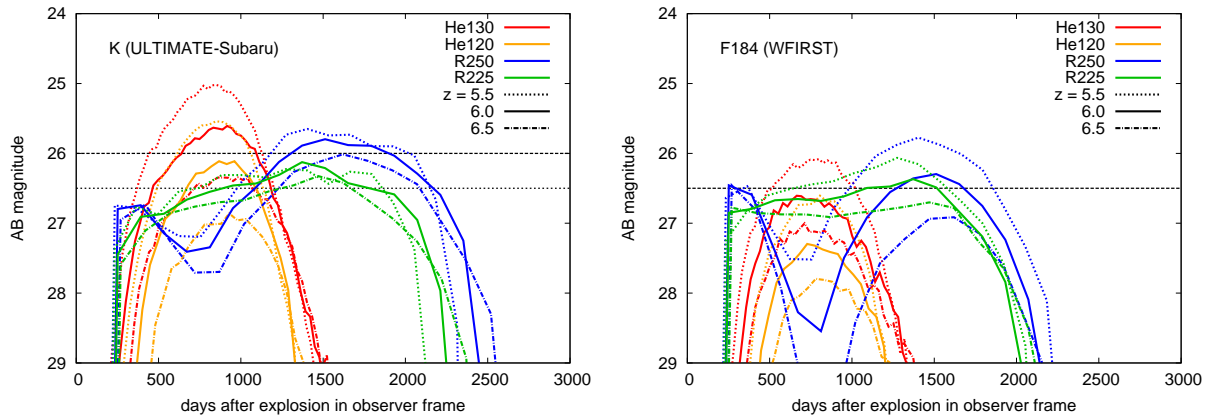


Fig. 2. Examples of PISN LCs adopted in our mock observation simulations. Left panel shows the K -band LCs expected for ULTIMATE-Subaru for which we assume the 26.0 mag and 26.5 mag limits (horizontal lines) in our survey simulations. Right panel shows the $F184$ -band LCs for WFIRST for which we assume the 26.5 mag limit (horizontal line) in the deepest survey simulations.

envelope and it is far from the central region where Fe-group elements locate. However, the helium core models have the photosphere at or close to where the ^{56}Ni is synthesized and they are more affected by absorption by the Fe-group elements.

R250 and R225 are the red supergiant (RSG) PISN progenitors with the ZAMS mass of $250 M_{\odot}$ and $225 M_{\odot}$, respectively. They have the initial metallicity of $10^{-4} Z_{\odot}$. The masses at the time of the explosion are $236 M_{\odot}$ (R250) and $200 M_{\odot}$ (R225) because of slight mass loss. A similar amount of mass loss is found even in the Pop III RSG PISN progenitors in Moriya & Langer (2015). Therefore, the RSG PISN LC properties are not likely to be much different from those of the zero-metallicity progenitors. He130 and He120 are the hydrogen-free PISN progenitors with the initial helium core masses of $130 M_{\odot}$ and $120 M_{\odot}$, respectively. It is the zero-metallicity (Pop III) models and the initial masses are kept until the time of the explosions without mass loss.

2.3.2 Rates

We adopt a PISN rate estimated by de Souza et al. (2014) in our mock observations (Fig. 3). de Souza et al. (2014) estimated the Pop III PISN rate based on the cosmological simulation of Johnson et al. (2013). We take the Pop III PISN rates estimated from their high SFR estimates (SFR10 in de Souza et al. 2014). de Souza et al. (2014) estimated Pop III PISN rate above $z = 6$. We also present the PISN discovery number estimates at $5 < z < 6$ by assuming that the PISN rate at $5 < z < 6$ is the same as that at $z = 6$.

There exist many works estimating the Pop III SFRs. Fig. 2 in de Souza et al. (2014) compares several predicted Pop III SFRs. The SFR10 model we adopt has a relatively high SFR prediction among others but other predictions stay roughly within a factor of 10 compared to the SFR10 estimate.

de Souza et al. (2014) assumed two initial mass functions

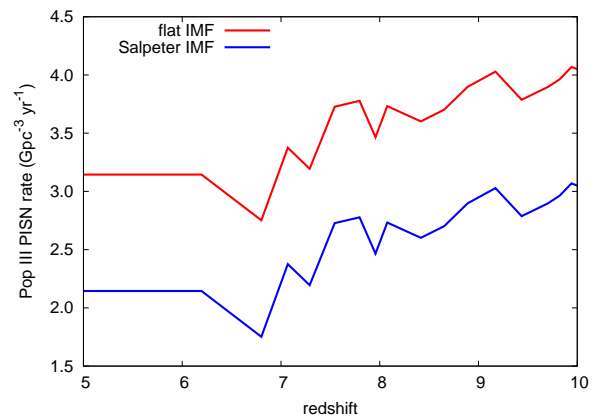


Fig. 3. Pop III PISN rate estimated by de Souza et al. (2014).

(IMFs) to estimate the Pop III PISN rate. One is the Salpeter IMF and the other is the flat IMF. The cosmological simulations of the first stars indicate that the IMF is close to the flat one in Pop III stars (Hirano et al. 2015).

The ZAMS mass range for Pop III PISNe is roughly between $140 M_{\odot}$ and $260 M_{\odot}$ (Heger & Woosley 2002). Only the R225 (ZAMS mass of $225 M_{\odot}$) and R250 (ZAMS mass of $250 M_{\odot}$) models in Pop III RSG PISN models of Kasen et al. (2011) become brighter than $K = 26.5$ mag and $F184 = 26.5$ mag when they appear at $z \gtrsim 6$. The R200 model (ZAMS mass of $200 M_{\odot}$) does not become bright enough. Kasen et al. (2011) does not provide RSG PISN LCs between $200 M_{\odot}$ and $225 M_{\odot}$ and we cannot tell the exact minimum ZAMS mass to be brighter than 26.5 mag. In this study, we assume that RSG Pop III PISNe whose ZAMS mass is above $215 M_{\odot}$ become bright enough to be observable at $z \sim 6$ with the $K = 26.5$ mag limit.

If we assume the $K = 26.0$ mag limit, the R225 model at $z \gtrsim 6$ cannot be observed and only R250 is observable. Similarly, Kasen et al. (2011) does not provide RSG PISN LCs

between $225 M_{\odot}$ and $250 M_{\odot}$ and we cannot tell the exact minimum ZAMS mass to be bright enough to observe with the limit. We assume that RSG Pop III PISNe whose ZAMS mass is above $240 M_{\odot}$ become bright enough to be observed at $z \sim 6$ with the $K = 26.0$ mag limit. We assume that the R250 LC is the representative LC of Pop III PISNe whose ZAMS masses are between $240 M_{\odot}$ and $260 M_{\odot}$ and the R225 LC is the representative LC of Pop III PISNe whose ZAMS masses are between $215 M_{\odot}$ and $240 M_{\odot}$.

If we assume the flat IMF, the fraction of Pop III PISNe with the ZAMS mass between $240 M_{\odot}$ and $260 M_{\odot}$ is 17%. In our mock observations, we thus assume that the R250 PISNe explode with the 17% rate of the total Pop III PISN rate obtained by de Souza et al. (2014) in the case of the flat IMF. Similarly, 21% of the Pop III PISN rate comes from between $215 M_{\odot}$ and $240 M_{\odot}$ with the flat IMF and we assume that the R225 PISNe occupies 21% of the Pop III IMF in case of the flat IMF. On the other hand, when we assume the Salpeter IMF, the PISN fraction in the ZAMS mass between $240 M_{\odot}$ and $260 M_{\odot}$ becomes 8.7% and the PISN fraction in the ZAMS mass between $215 M_{\odot}$ and $240 M_{\odot}$ becomes 14%. Therefore, we assume that the R250 model and the R225 model explode with the 8.7% and 14%, respectively, of the total PISN rate estimated by de Souza et al. (2014) in the case of the Salpeter IMF.

The bare helium core PISN models He120 and He130 are observable at $z \gtrsim 6$ with our deep surveys (Fig. 2). However, it is not obvious from which ZAMS masses these massive bare helium core progenitors originate (see Section 4.1 for discussion). Therefore, we perform mock observations only considering Pop III RSG PISN progenitors. We discuss the possible effect of helium core Pop III PISN progenitors in Section 4.

The blue supergiant (BSG) Pop III PISNe are not observable at $z \gtrsim 6$ with the $K = 26.5$ mag limit and a $F184 = 26.5$ mag limit. Many stellar evolution models predict that Pop III SLSNe with hydrogen explode as RSGs, not BSGs (e.g., Yoon et al. 2012; Moriya & Langer 2015). Therefore, we ignore Pop III BSG PISNe in this study.

2.4 Gravitational lensing

We also study the effect of the brightness magnification due to the gravitational lensing. Even if we observe a random field for the survey, the SN brightness could be amplified because of the galaxies happened to exist at the line of sight. To study the effect of the gravitational lensing towards the random field, we use the magnification probability distribution obtained by Hilbert et al. (2007) based on ray tracing calculations through the Millennium simulation (Springel et al. 2005). The distributions are updated versions that include the effect of baryons (Hilbert et al. 2008). As presented in Wong et al. (2019), we find the discrepancy between the magnification probability distribu-

tions estimated by the HSC SSP survey data and those estimated by using the simulation data. This discrepancy is likely from the incompleteness in the observational data and, therefore, we adopt the magnification probability distribution estimated based on the simulation.

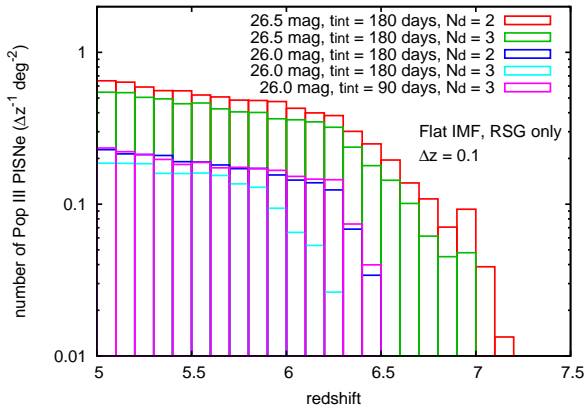
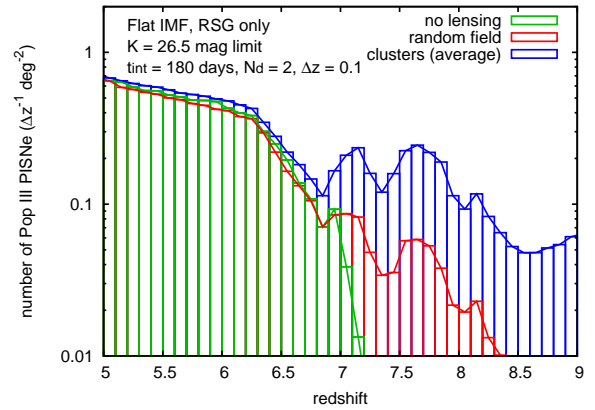
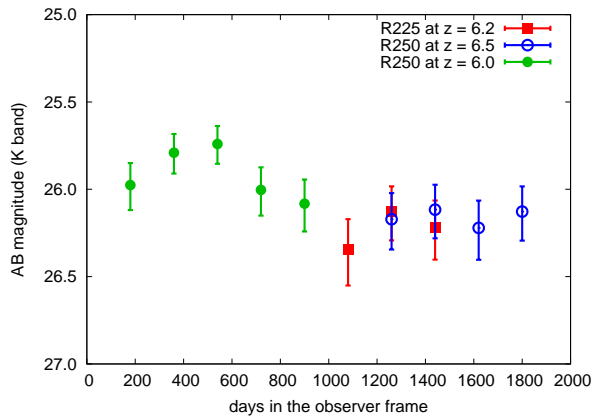
The probability of the magnification amplification can be significantly increased when the survey field is towards a massive cluster of galaxies. We refer to Wong et al. (2019) for the details of the cluster magnification calculations, but provide a brief summary here. We calculate the magnification distribution along lines of sight towards seven known massive ($M > 10^{15} M_{\odot}$) clusters of galaxies to estimate this effect and extrapolate it to our mock survey. These seven cluster models include the model of the massive cluster J0850+3604 from Wong et al. (2017), as well as models of the six *HST* Frontier Fields (Lotz et al. 2017) clusters from Kawamata et al. (2016); Kawamata et al. (2018) constructed using Oguri (2010). Both methods use parameterized models that account for both the cluster dark matter distribution and individual galaxies. We assume a $14' \times 14'$ field-of-view. We calculate the source plane area as a function of magnification for each of the seven clusters and take the average, extrapolated to the full area of our mock survey, to calculate the expected number of detections. This is somewhat optimistic, as these seven clusters are already among the most massive ones known, but there are potentially other clusters of similar mass that are relatively unexplored (e.g., Wong et al. 2013), and wide-area imaging surveys such as HSC, LSST, and Euclid could potentially find others. In regions of the source plane that are multiply-imaged, we take the magnification of the brightest image as the value at that particular location.

2.5 Simulation code

We use our own code to conduct mock observations to estimate the PISN detectability. The redshifts beyond 5 are binned with $\Delta z = 0.1$ and PISNe are assumed to appear in each redshift bin with the PISN rates estimated in the previous section. Once a PISN appears at a redshift bin, the apparent magnitudes in the observer frame at the time of the observation that is determined by t_{int} and the observational period are evaluated. For this purpose, we use redshifted PISN LCs that are calculated based on the PISN spectral model of Kasen et al. (2011) in advance for each redshifts. We check the expected observations and judge if the observations match our criteria, such as the limiting magnitudes and N_{d} , to regard them as a discovery. When we take the gravitational lensing effect into account, we randomly change PISN magnitudes based on the assumed magnification probability distribution.

Table 1. Numbers of Pop III RSG PISN discoveries for the 5-year survey without the gravitational lensing effect.

band	FoV deg ²	limit mag	t_{int} days	N_d	flat IMF			Salpeter IMF		
					$z > 5$	$z > 6$	$z > 7$	$z > 5$	$z > 6$	$z > 7$
K^a	1	26.5	180	2	7.9 ± 0.4	2.4 ± 0.2	0.06 ± 0.03	0.4 ± 0.1	0.13 ± 0.05	0.005 ± 0.002
	1	26.5	180	3	6.4 ± 0.5	1.8 ± 0.3	0.008 ± 0.004	0.35 ± 0.09	0.09 ± 0.04	0
	2	26.0	180	2	4.9 ± 0.4	1.0 ± 0.2	0	0.24 ± 0.06	0.04 ± 0.02	0
	2	26.0	180	3	3.4 ± 0.2	0.3 ± 0.1	0	0.3 ± 0.1	0.006 ± 0.04	0
	2	26.0	90	3	5.0 ± 0.4	1.2 ± 0.2	0	0.24 ± 0.06	0.04 ± 0.04	0
$F184^b$	1	27.0	180	2	10.6 ± 0.3	4.4 ± 0.2	1.10 ± 0.08	0.60 ± 0.05	0.24 ± 0.03	0.06 ± 0.01
	10	26.5	180	2	57 ± 2	6.8 ± 0.7	0	3.2 ± 0.4	0.3 ± 0.1	0
	10	26.0	180	2	13.2 ± 0.6	0	0	0.7 ± 0.1	0	0

^aULTIMATE-Subaru, ^bWFIRST**Fig. 4.** Differences in Pop III PISN discoveries from the different survey parameters with ULTIMATE-Subaru.**Fig. 6.** Effect of the magnitude amplification due to gravitational lensing.**Fig. 5.** Examples of Pop III PISN LCs observed by the $t_{\text{int}} = 180$ days survey with a 26.5 mag limit in the K band with ULTIMATE-Subaru.

3 Results

Mock transient surveys with one condition are repeated 100 times to check statistical errors. All the errors shown in the following number estimates are the 1σ statistical errors.

3.1 ULTIMATE-Subaru

Table 1 summarizes the numbers of Pop III RSG PISNe discovered in our mock transient surveys with several observational strategies. Fig. 4 shows the redshift distributions of the observed Pop III RSG PISNe in the case of the flat IMF. The examples of the observed Pop III PISN LCs for the survey with $t_{\text{int}} = 180$ days are presented in Fig. 5.

We find that $t_{\text{int}} = 180$ days works well to find Pop III PISNe at $z \gtrsim 6$. If we set the survey FoV to be 1 deg^2 in the 26.5 mag surveys (860 hours in total with $t_{\text{int}} = 180$ days) and 2 deg^2 in the 26.0 mag surveys (960 hours in total with $t_{\text{int}} = 180$ days), we predict to find a few Pop III PISNe at $z \gtrsim 6$ during the 5-year survey if the IMF is flat. If we assume the Salpeter IMF, the expected number of RSG Pop III PISN detections is as low as ~ 0.1 in the whole survey.

The 26.5 mag limit surveys are predicted to find much more Pop III RSG PISNe because the deeper surveys can find less massive Pop III PISN progenitors. Comparing the 26.0 mag 2 deg^2 survey that takes about 960 hours with the 26.5 mag 1 deg^2 survey that takes about 860 hours, having a deeper survey with a smaller FoV is likely beneficial to find Pop III PISNe than having a shallower survey with a larger FoV (Table 1).

Table 2. Numbers of RSG Pop III PISN discoveries for the ULTIMATE-Subaru 5-year 1-deg^2 $t_{\text{int}} = 180$ days $N_d = 2$ survey with gravitational lensing.

source	$z > 5$	$z > 6$	$z > 7$
$K = 26.5$ mag limit			
no lensing	7.9 ± 0.4	2.4 ± 0.2	0.06 ± 0.03
random field	8.1 ± 0.4	2.9 ± 0.2	0.7 ± 0.1
cluster average	12.2 ± 1.7	6.4 ± 1.5	3.6 ± 1.3
$K = 26.0$ mag limit			
no lensing	2.4 ± 0.2	0.52 ± 0.08	0
random field	2.9 ± 0.2	0.61 ± 0.09	0.08 ± 0.03
cluster average	5.5 ± 1.1	2.2 ± 0.8	1.1 ± 0.6

The expected number of Pop III RSG PISN discoveries can be enhanced if we perform the transient survey towards clusters of galaxies. Table 2 and Fig. 6 summarize the expected numbers of Pop III RSG PISN discoveries obtained by adopting the gravitational amplification probability distributions (see Section 2.4 for details). We focus the $K = 26.5$ mag survey with $t_{\text{int}} = 180$ days and $N_d = 2$ in this study to present the possibility to reach very high redshifts by the gravitational lensing by clusters of galaxies. We find that the cluster lensing roughly doubles the expected number of Pop III RSG PISN detections at $z > 6$. We also find that the cluster lensing significantly increases the chance to observe PISNe at $z > 7$ as seen in Fig. 6. The bumps in the detection numbers come from the bumps in the Pop III PISN rates (Fig. 3).

3.2 WFIRST

Table 1 presents the WFIRST Pop III RSG PISN discoveries and Figure 7 shows their redshift distributions. Although WFIRST does not reach as red as ULTIMATE-Subaru, it can easily reach deeper limiting magnitudes thanks to being in space. We find that the $F184$ -band survey with the limiting magnitude of 26.5 mag with WFIRST can discover PISNe as distant as the K -band survey with the limiting magnitude of 26.0 mag with ULTIMATE-Subaru can do is. If we compare the same limiting magnitude survey with WFIRST and ULTIMATE-Subaru, ULTIMATE-Subaru can reach higher redshifts thanks to its redder band. However, WFIRST can reach deeper limiting magnitudes rather easily and the WFIRST survey with the limiting magnitude of 27.0 mag can go beyond the ULTIMATE-Subaru survey with the limiting magnitude of 26.5 mag.

4 Discussion

4.1 Helium core PISNe

Pop III PISN discovery estimates in the previous section do not take helium core PISN progenitors into account. One possible

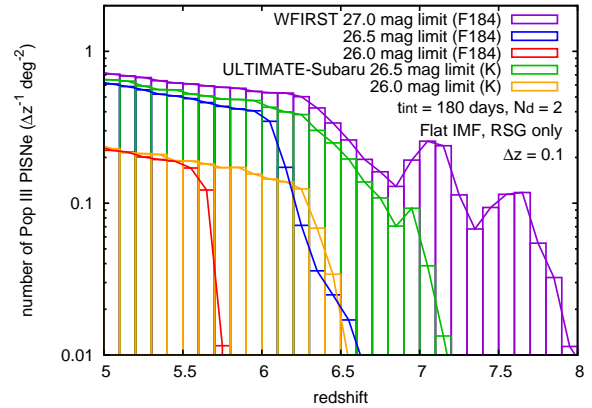


Fig. 7. Results of the WFIRST Pop III RSG PISN mock surveys. The numbers are per deg^2 and the actual discovery numbers are proportional to the survey area.

path for helium core Pop III PISNe to appear is by stripping the envelope of massive RSG PISN progenitors through, e.g., binary interaction. The helium core mass of the R250 model is $124 M_{\odot}$ (Kasen et al. 2011). Because helium core PISNe with the helium core mass above $\approx 125 M_{\odot}$ is able to observe in our surveys (Section 2.3.2), Pop III massive stars with the ZAMS masses of $\sim 250 M_{\odot}$, which are observable if they explode as RSGs, may not be observable if they explode as helium stars. Thus, the expected detection number could go down if some massive RSG Pop III PISN progenitors explode as bare helium core Pop III PISNe.

On the other hand, bare helium core Pop III PISN progenitors can originate from massive stars with relatively low ZAMS mass (e.g., Chatzopoulos & Wheeler 2012). For example, if massive stars rotate rapidly, the rapid rotations can enhance the internal chemical mixing in massive stars and they could evolve chemically homogeneously (Yoon & Langer 2005). In this case, the ZAMS mass of the He130 progenitor could be as low as $\sim 130 M_{\odot}$. Interestingly enough, a large fraction of Pop III massive stars might be rapidly rotating stars (Hirano & Bromm 2018). Close binary systems could also make massive stars to evolve through the chemically homogeneous channel (e.g., Marchant et al. 2016). It is also possible that rapidly rotating massive stars originate from mergers of two low mass stars (e.g., van den Heuvel & Portegies Zwart 2013).

In summary, it is currently very hard to quantify how the bare helium core PISN channel would affect the PISN detectability. We speculate that the expected RSG Pop III discovery number we discussed in the previous section could be lower limits because of the many possible ways to make relatively low mass massive stars to be massive enough to explode as bare helium core PISN progenitors. However, we speculate that the K band survey with ULTIMATE-Subaru is much better to detect the helium core PISNe because of their faintness in the $F184$ band

(Fig. 2). In this sense, ULTIMATE-Subaru has an advantage to find different kinds of Pop III PISNe.

4.2 Pop II PISNe

We have focused on Pop III PISN discoveries in this study. At $z \sim 6$, however, Pop II SFR is expected to be ~ 100 higher than Pop III SFR (e.g., Wise et al. 2012). On the other hand, Pop II IMF might be closer to the Salpeter IMF than the flat IMF we mainly focused in our Pop III study. If Pop II IMF is approximated as the Salpeter IMF and Pop II PISN properties are similar to Pop III PISN properties, we would roughly expect about 100 times more PISNe than the Pop III PISN number estimates for the Salpeter IMF. This means that we typically expect to detect about 10 or more Pop II PISNe at $z \sim 6$ in our deepest surveys with ULTIMATE-Subaru and WFIRST if Pop II PISNe follows the Salpeter IMF (see Table 1). Thus, in addition to several Pop III PISNe, we might be able to find many Pop II PISNe in the deep NIR transient surveys with ULTIMATE-Subaru and WFIRST.

4.3 SLSNe

NIR transient surveys discussed in this paper not only have capabilities to find Pop III PISNe but also high-redshift SLSNe. Detectability of high-redshift SLSNe with WFIRST was estimated in Tanaka et al. (2013). By scaling their results, we expect to detect ~ 10 SLSNe at $z \gtrsim 1$, including a few SLSNe at $z \gtrsim 6$, with a 1 deg^2 and 26 mag limit survey in NIR. A similar number is expected for a 1 deg^2 and 26.5 mag limit survey.

4.4 Identifying Pop III PISNe

We have shown that discovering Pop III PISNe is possible by performing the proper transient surveys using ULTIMATE-Subaru and WFIRST. However, in order to confirm the Pop III PISN discovery, it is necessary to follow up the PISN candidates. In the era of ULTIMATE-Subaru and WFIRST operations, we expect that James Webb Space Telescope (JWST) and several 30-m class telescopes such as Thirty Meter Telescope (TMT) are under operation and they will be essential tools for the spectroscopic follow up.

Even with these follow-up facilities, it is important to consider how to select the Pop III PISN candidates to follow. The LCs obtained during the survey are already very important information but having several other information is also important. Especially, we have assumed the NIR transient surveys in a single filter here and we do not have color information to select good Pop III PISN candidates. Performing the NIR transient surveys in a few filters are the best option, but it is also likely that we can perform the transient survey only in a single filter

because of the limited telescope time. In this respect, conducting a coordinated simultaneous observational campaign with the same field with ULTIMATE-Subaru and WFIRST is the best option to have both the K band and $F184$ band information. It is also helpful to have simultaneous optical observations in the same field for the efficient candidate selection, because high-redshift SNe should be faint in optical. These photometric information can be processed by using SN photometric classification methods to search for genuine PISNe. Recently, SN photometric classification schemes have been developing quickly to prepare for the coming era of extensive time domain surveys with, e.g., Large Synoptic Survey Telescope³ (e.g., Ishida et al. 2019; Ishida & de Souza 2013; Charnock & Moss 2017; Möller & de Boissière 2019). They will be essential to reject many contaminants such as SNe Ia and core-collapse SNe at low redshifts. They can also be trained by using the PISN LC models to directly identify the high-redshift PISN candidates. Having multi-band information including both optical and NIR is also helpful when we adopt photometric classification methods.

Another important information is provided by the host galaxies. If we perform a transient survey with legacy data from many wavelengths such as the COSMOS field, we can use the preexisting host galaxy information to estimate their photometric redshifts, for example. The host galaxy photometric redshifts are found to be useful in finding high-redshift SNe (e.g., Moriya et al. 2019; Curtin et al. 2019). In order to identify $z \gtrsim 6$ galaxies photometrically, we can look for "dropout" galaxies (e.g., Steidel et al. 1999; Ono et al. 2018). Galaxies at $z \sim 6$ are observed as " i -dropout" galaxies and those at $z \sim 7 - 9$ are observed as " z -dropout" or " Y -dropout" galaxies. Deep NIR images are required in advance for the identification of these dropout galaxies.

5 Conclusions

We have performed mock NIR transient surveys with ULTIMATE-Subaru and WFIRST to estimate their expected numbers of Pop III PISN detections at $z \gtrsim 6$. We adopt Pop III PISN rates estimated based on the cosmological simulations by de Souza et al. (2014) and used the Pop III PISN LC models by Kasen et al. (2011). We found that a few Pop III PISNe at $z \gtrsim 6$ may be detected if we perform the 1 deg^2 K -band ULTIMATE-Subaru transient survey for 5 years with the limiting magnitude of 26.5 mag (860 hours in total), assuming the flat IMF for Pop III stars. If we assume the Salpeter IMF, the expected number is decreased by a factor of 10. If we set the limiting magnitude to be 26.0 mag, we expect about 1 Pop III PISN detection with the 2 deg^2 survey (960 hours in total). We found that the expected numbers of the Pop III discovery will be doubled if the transient surveys are conducted towards clus-

³ <https://www.lsst.org/>

ters of galaxies thanks to the magnification by the gravitational lensing.

The reddest filter of WFIRST ($F184$) is bluer than that of ULTIMATE-Subaru (K). However, WFIRST has the larger FoV than ULTIMATE-Subaru and it allows to conduct wider transient surveys. If we conduct the 5-year transient survey with the $F184$ filter with the limiting magnitude of 26.5 mag for 10 deg² (200 hours), we expect to find about 7 Pop III PISNe with the flat IMF and about 0.3 Pop III PISNe with the Salpeter IMF.

Our study has shown that the deep and wide NIR transient surveys conducted by the planned wide-field NIR imagers will enable us to acquire valuable information on the first generation stars in the Universe. They have a possibility to find Pop III PISNe. Even if we do not discover any Pop III PISNe, such NIR transient surveys will enable us to constrain the star-formation properties like IMF of the first stars.

Acknowledgments

TJM thanks horrible weather at Mauna Kea in Feb and Mar 2018 which led to the cancellation of his Subaru observations that made this study done. We thank Dan Kasen for sharing electric data of PISN LC models. TJM thanks Chien-Hsiu Lee for discussion. TJM is supported by the Grants-in-Aid for Scientific Research of the Japan Society for the Promotion of Science (16H07413, 17H02864, 18K13585). KCW is supported in part by an EACOA Fellowship awarded by the East Asia Core Observatories Association, which consists of the Academia Sinica Institute of Astronomy and Astrophysics, the National Astronomical Observatory of Japan, the National Astronomical Observatories of the Chinese Academy of Sciences, and the Korea Astronomy and Space Science Institute. MO is supported in part by JSPS KAKENHI Grant Number JP15H05892 and JP18K03693.

This work was supported by World Premier International Research Center Initiative (WPI Initiative), MEXT, Japan.

The Hyper Suprime-Cam (HSC) collaboration includes the astronomical communities of Japan and Taiwan, and Princeton University. The HSC instrumentation and software were developed by the National Astronomical Observatory of Japan (NAOJ), the Kavli Institute for the Physics and Mathematics of the Universe (Kavli IPMU), the University of Tokyo, the High Energy Accelerator Research Organization (KEK), the Academia Sinica Institute for Astronomy and Astrophysics in Taiwan (ASIAA), and Princeton University. Funding was contributed by the FIRST program from Japanese Cabinet Office, the Ministry of Education, Culture, Sports, Science and Technology (MEXT), the Japan Society for the Promotion of Science (JSPS), Japan Science and Technology Agency (JST), the Toray Science Foundation, NAOJ, Kavli IPMU, KEK, ASIAA, and Princeton University.

The Pan-STARRS1 Surveys (PS1) have been made possible through contributions of the Institute for Astronomy, the University of Hawaii, the Pan-STARRS Project Office, the Max-Planck Society and its participating institutes, the Max Planck Institute for Astronomy, Heidelberg and the Max Planck Institute for Extraterrestrial Physics, Garching, The Johns Hopkins University, Durham University, the University of Edinburgh, Queen's University Belfast, the Harvard-Smithsonian Center for Astrophysics, the Las Cumbres Observatory Global Telescope Network Incorporated, the National Central University of Taiwan, the Space Telescope Science Institute, the National Aeronautics and Space

Administration under Grant No. NNX08AR22G issued through the Planetary Science Division of the NASA Science Mission Directorate, the National Science Foundation under Grant No. AST-1238877, the University of Maryland, and Eotvos Lorand University (ELTE).

This paper makes use of software developed for the Large Synoptic Survey Telescope. We thank the LSST Project for making their code available as free software at <http://dm.lsst.org>.

Based in part on data collected at the Subaru Telescope and retrieved from the HSC data archive system, which is operated by the Subaru Telescope and Astronomy Data Center at National Astronomical Observatory of Japan.

References

- Barkat, Z., Rakavy, G., & Sack, N. 1967, *Physical Review Letters*, 18, 379
- Chambers, K. C., et al. 2016, ArXiv e-prints, arXiv:1612.05560
- Charnock, T., & Moss, A. 2017, *ApJL*, 837, L28
- Chatzopoulos, E., & Wheeler, J. C. 2012, *ApJ*, 748, 42
- Curtin, C., et al. 2019, ArXiv e-prints, arXiv:1801.08241
- de Souza, R. S., Ishida, E. E. O., Johnson, J. L., Whalen, D. J., & Mesinger, A. 2013, *MNRAS*, 436, 1555
- de Souza, R. S., Ishida, E. E. O., Whalen, D. J., Johnson, J. L., & Ferrara, A. 2014, *MNRAS*, 442, 1640
- Dessart, L., Hillier, D. J., Waldman, R., Livne, E., & Blondin, S. 2012, *MNRAS*, 426, L76
- Gal-Yam, A., et al. 2009, *Nature*, 462, 624
- Georgy, C., Meynet, G., Ekström, S., Wade, G. A., Petit, V., Keszthelyi, Z., & Hirschi, R. 2017, *A&A*, 599, L5
- Hartwig, T., Bromm, V., & Loeb, A. 2018, *MNRAS*, arXiv:1711.05742
- Heger, A., & Woosley, S. E. 2002, *ApJ*, 567, 532
- Hilbert, S., White, S. D. M., Hartlap, J., & Schneider, P. 2007, *MNRAS*, 382, 121
- , 2008, *MNRAS*, 386, 1845
- Hirano, S., & Bromm, V. 2018, *MNRAS*, 476, 3964
- Hirano, S., Hosokawa, T., Yoshida, N., Omukai, K., & Yorke, H. W. 2015, *MNRAS*, 448, 568
- Hounsell, R., et al. 2017, ArXiv e-prints, arXiv:1702.01747
- Ichikawa, T., et al. 2006, in *Proc. SPIE*, Vol. 6269, Society of Photo-Optical Instrumentation Engineers (SPIE) Conference Series, 626916
- Inserra, C., et al. 2017, ArXiv e-prints, arXiv:1710.09585
- Ishida, E. E. O., & de Souza, R. S. 2013, *MNRAS*, 430, 509
- Ishida, E. E. O., et al. 2019, *MNRAS*, 483, 2
- Jerkstrand, A., Smartt, S. J., & Heger, A. 2016, *MNRAS*, 455, 3207
- Johnson, J. L., Dalla Vecchia, C., & Khochfar, S. 2013, *MNRAS*, 428, 1857
- Kasen, D., Woosley, S. E., & Heger, A. 2011, *ApJ*, 734, 102
- Kasliwal, M. M., et al. 2017, *ApJ*, 839, 88
- Kawamata, R., Ishigaki, M., Shimasaku, K., Oguri, M., Ouchi, M., & Tanigawa, S. 2018, *ApJ*, 855, 4
- Kawamata, R., Oguri, M., Ishigaki, M., Shimasaku, K., & Ouchi, M. 2016, *ApJ*, 819, 114
- Keller, S. C., et al. 2007, *PASA*, 24, 1
- Kool, E. C., et al. 2018, *MNRAS*, 473, 5641
- Kozyreva, A., et al. 2016, *MNRAS*, arXiv:1610.01086
- Langer, N. 2012, *ARA&A*, 50, 107
- Langer, N., Norman, C. A., de Koter, A., Vink, J. S., Cantiello, M., &

- Yoon, S.-C. 2007, *A&A*, 475, L19
- Law, N. M., et al. 2009, *PASP*, 121, 1395
- Lotz, J. M., et al. 2017, *ApJ*, 837, 97
- Marchant, P., Langer, N., Podsiadlowski, P., Tauris, T. M., & Moriya, T. J. 2016, *A&A*, 588, A50
- Mattila, S., et al. 2012, *ApJ*, 756, 111
- Möller, A., & de Boissière, T. 2019, arXiv e-prints, arXiv:1901.06384
- Moriya, T. J., & Langer, N. 2015, *A&A*, 573, A18
- Moriya, T. J., Sorokina, E. I., & Chevalier, R. A. 2018, *Space Sci. Rev.*, 214, 59
- Moriya, T. J., et al. 2019, ArXiv e-prints, arXiv:1801.08240
- Morokuma, T., et al. 2014, *PASJ*, 66, 114
- Oguri, M. 2010, *PASJ*, 62, 1017
- Ono, Y., et al. 2018, *PASJ*, 70, S10
- Quimby, R. M., et al. 2011, *Nature*, 474, 487
- Rakavy, G., & Shaviv, G. 1967, *ApJ*, 148, 803
- Scannapieco, E., Madau, P., Woosley, S., Heger, A., & Ferrara, A. 2005, *ApJ*, 633, 1031
- Smith, N., et al. 2007, *ApJ*, 666, 1116
- Spergel, D., et al. 2015, ArXiv e-prints, arXiv:1503.03757
- Springel, V., et al. 2005, *Nature*, 435, 629
- Steidel, C. C., Adelberger, K. L., Giavalisco, M., Dickinson, M., & Pettini, M. 1999, *ApJ*, 519, 1
- Suzuki, R., et al. 2008, *PASJ*, 60, 1347
- Tanaka, M., Moriya, T. J., & Yoshida, N. 2013, *MNRAS*, 435, 2483
- Tanaka, M., et al. 2016, *ApJ*, 819, 5
- Tolstov, A., Zhiglo, A., Nomoto, K., Sorokina, E., Kozyreva, A., & Blinnikov, S. 2017, *ApJL*, 845, L2
- Umeda, H., & Nomoto, K. 2002, *ApJ*, 565, 385
- van den Heuvel, E. P. J., & Portegies Zwart, S. F. 2013, *ApJ*, 779, 114
- Whalen, D. J., Smidt, J., Rydberg, C.-E., Johnson, J. L., Holz, D. E., & Stiavelli, M. 2013a, arXiv e-prints, arXiv:1312.6330
- Whalen, D. J., et al. 2013b, *ApJ*, 777, 110
- . 2014, *ApJ*, 797, 9
- Wise, J. H., Turk, M. J., Norman, M. L., & Abel, T. 2012, *ApJ*, 745, 50
- Wong, K. C., Moriya, T. J., Oguri, M., Hilbert, S., & Koyama, Y. 2019, *PASJ*, submitted
- Wong, K. C., Raney, C., Keeton, C. R., Umetsu, K., Zabludoff, A. I., Ammons, S. M., & French, K. D. 2017, *ApJ*, 844, 127
- Wong, K. C., Zabludoff, A. I., Ammons, S. M., Keeton, C. R., Hogg, D. W., & Gonzalez, A. H. 2013, *ApJ*, 769, 52
- Yoon, S.-C., Dierks, A., & Langer, N. 2012, *A&A*, 542, A113
- Yoon, S.-C., & Langer, N. 2005, *A&A*, 443, 643
- Yoshida, T., Okita, S., & Umeda, H. 2014, *MNRAS*, 438, 3119